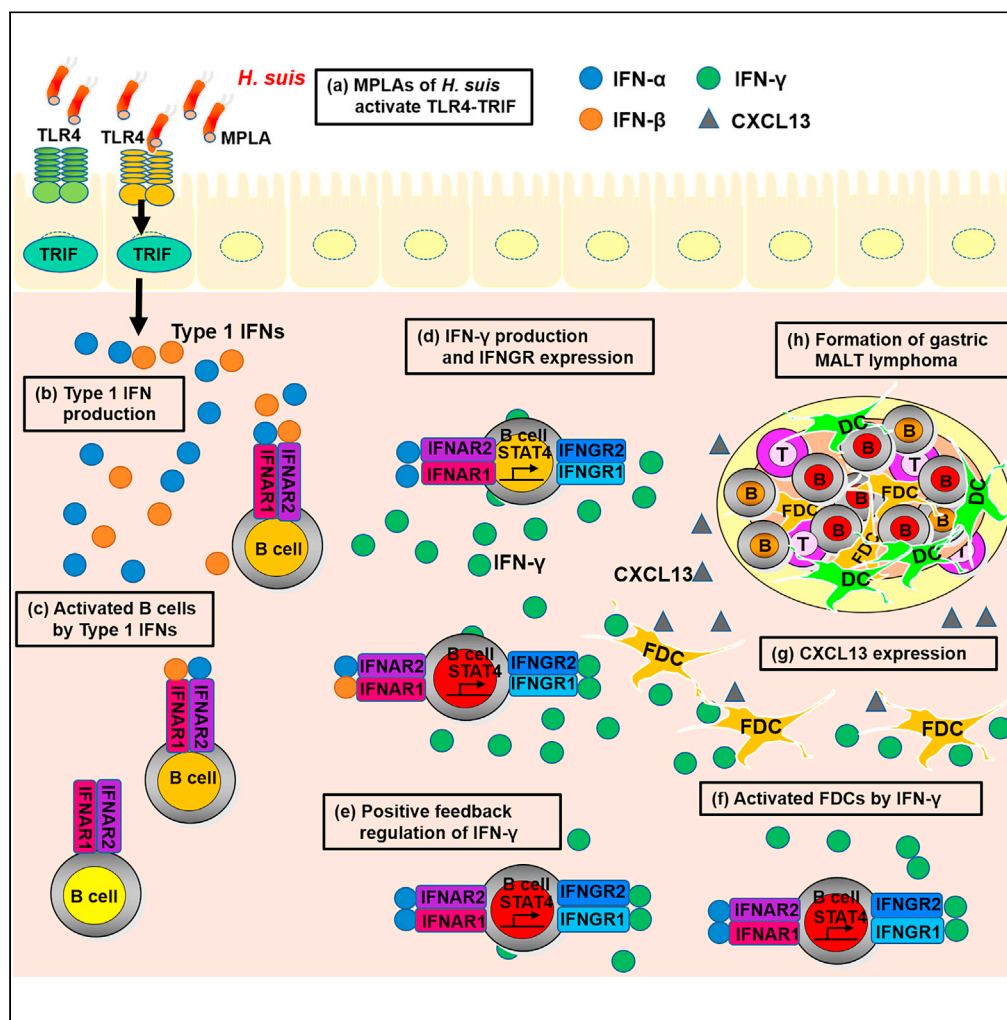**Article**

# The TLR4–TRIF–type 1 IFN–IFN-γ pathway is crucial for gastric MALT lymphoma formation after *Helicobacter suis* infection



Koji Yamamoto,
Yasuyuki Kondo,
Shunsuke Ohnishi,
Masaru Yoshida,
Toshiro Sugiyama,
Naoya Sakamoto

kyama@pop.med.hokudai.ac.jp

**Highlights**

*H. suis* MPLA causes type 1 IFN production in the stomach via TLR4–TRIF signaling

The interaction between type 1 IFNs and IFNAR on B cells causes IFN-γ production

Interaction of IFN-γ and IFNGR on B cells causes IFN-γ positive feedback regulation

IFN-γ from gastric B cells induces gastric lymphoid follicles after *H. suis* infection

Article

# The TLR4–TRIF–type 1 IFN–IFN-γ pathway is crucial for gastric MALT lymphoma formation after *Helicobacter suis* infection

Koji Yamamoto,[1,2,5,*] Yasuyuki Kondo,[3] Shunsuke Ohnishi,[2] Masaru Yoshida,[3,4] Toshiro Sugiyama,[1] and Naoya Sakamoto[2]

## SUMMARY

***Helicobacter suis*, a zoonotic infection-related bacterium, can induce gastric mucosa-associated lymphoid tissue (MALT) lymphoma in humans and animals. Recently, we reported that the formation of gastric MALT lymphoma after *H. suis* infection is induced by interferon (IFN)-γ activation. Here, we revealed that activation of the Toll-like receptor (TLR) 4–Toll/IL-1 receptor domain-containing adapter-inducing interferon-β (TRIF) pathway after *H. suis* infection is associated with the production of type 1 IFNs (IFN-α, IFN-β) by gastric epithelial cells. Additionally, these type 1 IFNs interact with type 1 IFN receptors on gastric B cells, facilitating the secretion of IFN-γ and the activation of which is enhanced by positive feedback regulation in B cells. These results suggest that the TLR4–TRIF-type 1 IFN–IFN-γ pathway is crucial in the development of gastric MALT lymphoma after *H. suis* infection and may, therefore, represent a therapeutic target for the prevention of this condition.**

## INTRODUCTION

*Helicobacter suis*, similar to *Helicobacter pylori*, is a fastidious gram-negative bacterium that colonizes the stomach of humans and various animals, such as pigs, dogs, and cats (O'Rourke et al., 2004; Priestnall et al., 2004; Yamamoto et al., 2011) and is strongly associated with gastric mucosa-associated lymphoid tissue (MALT) lymphoma (Nakamura et al., 2007; Okumura et al., 2013). Recently, our group reported that interferon (IFN)-γ, produced by infiltrating gastric B cells after *H. suis* infection, is important for gastric lymphoid follicle formation; in fact, IFN-γ-producing B cells are self-sufficient and function independently of T cells, dendritic cells (DCs), and follicular DCs (FDCs), suggesting their crucial role in developing gastric MALT lymphoma after *H. suis* infection (Yang et al., 2015).

Toll-like receptors (TLRs) are transmembrane proteins that play a critical role in the recognition of microbial components and IFN production (Medzhitov and Janeway, 1998; Aderem and Ulevitch, 2000; Imler and Hoffmann, 2001). TLR4 was the first identified pattern-recognition receptor with a specific ligand (Hoshino et al., 1999) on the cell surface of monocytes/macrophages (Nakao et al., 2005; Hansen et al., 2015). TLR4 signaling is involved in two downstream pathways, the myeloid differentiation factor 88 (MyD88) and the Toll/IL-1 receptor-domain-containing adapter-inducing interferon-β (TRIF) pathways (Takeda and Akira, 2005). IFN-β induction via TLR4 depends mostly on the TRIF pathway, whereas proinflammatory cytokine production depends on the MyD88 and TRIF pathways (Takeda and Akira, 2005). Patients with *H. pylori* infection express TLR4 in the gastric mucosa (Schmausser et al., 2004; Asahi et al., 2007), which may be involved in gastric diseases. Unlike other stomach-infiltrating lymphomas (Adam et al., 2008), MALT-type gastric extranodal marginal zone B cell lymphomas exclusively express TLR4, suggesting that TLR4-related signaling is important for gastric MALT lymphoma formation after *Helicobacter suis* infection.

We recently reported that *H. suis* infection induces gastric B cells to produce IFN-γ, which results in the formation of gastric lymphoid follicles (Yang et al., 2015). However, the mechanism of IFN-γ production induced by *H. suis* infection and its involvement in gastric lymphoid follicle formation remain unclear. Based on the current knowledge, we hypothesized that TLR4 signaling and IFN-γ production are linked and together contribute to the formation of gastric MALT lymphoma after *Helicobacter* infection. In this study, we revealed that type 1 IFNs are induced by activation of the TLR4–TRIF pathway in gastric epithelial cells

[1]Research Division of Molecular Targeting Therapy and Prevention of GI Cancer, Hokkaido University Hospital, Sapporo, Hokkaido 060-8638, Japan

[2]Department of Gastroenterology and Hepatology, Hokkaido University Graduate School of Medicine, Sapporo, Hokkaido 060-8638, Japan

[3]Division of Gastroenterology, Department of Internal Medicine, Kobe University Graduate School of Medicine, Kobe, Hyogo 650-0017, Japan

[4]Division of Metabolomics Research, Kobe University Graduate School of Medicine, Kobe, Hyogo 650-0017, Japan

[5]Lead contact
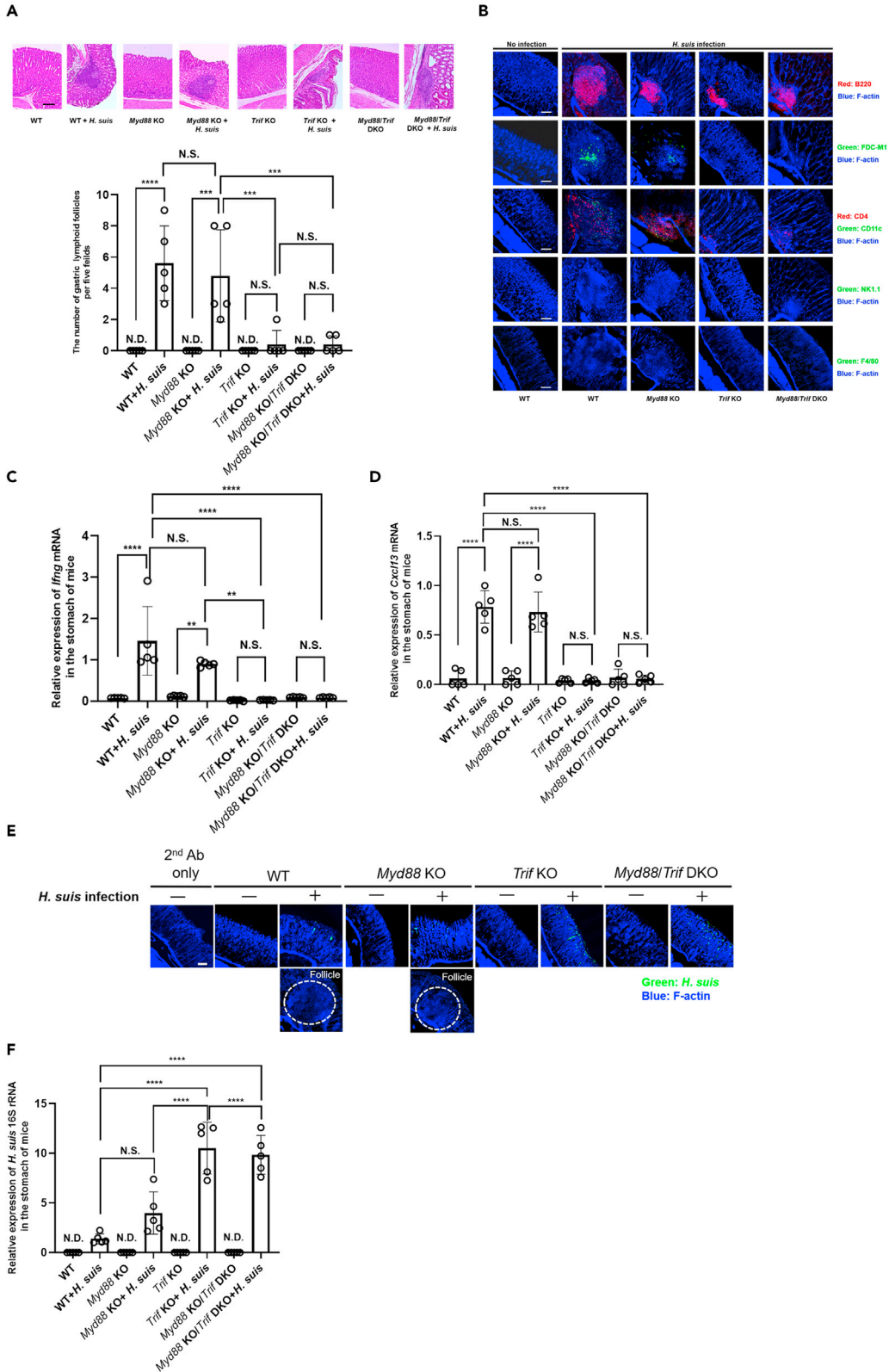
*Correspondence: kyama@pop.med.hokudai.ac.jp

https://doi.org/10.1016/j.isci.2021.103064

**Figure 1. Formation of gastric lymphoid follicles after *Helicobacter suis* infection**

C57BL/6J WT, *Myd88* KO, *Trif* KO, and *Myd88*/*Trif* DKO mice (n = 5 each) were analyzed 6 months after *H. suis* infection.

(A) Histological examination and mean number of gastric lymphoid follicles. Original magnification, 200×.

(B) Immunohistology of immunocompetent cells in the stomach (n = 5 each group). B220-positive cells (B cells), CD4-positive cells (helper T cells), CD11c-positive cells (dendritic cells; DCs), follicular dendritic cells (FDCs), NK1.1-positive cells (natural killer cells), and phalloidin (F-actin) were analyzed with confocal microscopy. Magnification, 100×.

*Ifng* (C) and *Cxcl13* (D) mRNA levels determined with qRT-PCR.

(E) Immunohistology of *H. suis* distribution (n = 5 each) via confocal microscopy. Magnification, 100×.

(F) *H. suis* 16S rRNA levels determined with qRT-PCR. (C, D, and F) Quantitative values were normalized to mouse β-actin levels (n = 5).

Data are shown as the mean ± SD of three independent experiments. *p < 0.05, **p < 0.01, N.S., no significant difference (ANOVA). DKO, double knockout; N.D., not detected. Scale bar, 100 μm.

after *H. suis* infection and can induce the production of IFN-γ from gastric B cells via an interaction between type 1 IFNs and type 1 IFN receptors (IFNARs). Therefore, blockade of the TLR4–TRIF signaling pathway is expected to effectively inhibit gastric MALT lymphoma development following *Helicobacter* infection.

## RESULTS

### TRIF pathway activation is crucial for the development of gastric lymphoid follicles after *H. suis* infection

Previous reports have suggested that MyD88 and TRIF are crucial adaptor proteins for TLR4 signaling and IFN production (Takeda and Akira, 2005). In this study, C57BL/6J (wild-type [WT] mice), *Myd88* knockout (KO), *Trif* KO, and *Myd88*/*Trif* double knockout (DKO) mice were infected with *H. suis* for 6 months to investigate the roles of these proteins in the formation of gastric lymphoid follicles. We detected gastric MALT lymphoma formation mainly in the stomachs of *H. suis*-infected WT and *Myd88* KO mice compared with that in the stomachs of *Trif* KO and *Myd88*/*Trif* DKO mice (Figure 1A). To determine the immunocompetent cells infiltrating follicles after *H. suis* infection, immunofluorescence staining was performed using appropriate antibodies. Consistent with our recent reports (Yamamoto et al., 2014; Yang et al., 2015), B cells, CD4+ T cells, DCs, and FDCs, but not natural killer cells and monocytes/macrophages, were identified in the gastric lymphoid follicles of *H. suis*-infected WT and *Myd88* KO mice, and several gastric MALT lymphomas were observed in these animals. In contrast, the infiltration of these cells was decreased in the *H. suis*-infected *Trif* KO and *Myd88*/*Trif* DKO mice, with fewer follicles detected (Figure 1B). These results suggest that the TRIF pathway plays a crucial role in the formation of gastric lymphoid follicles after *H. suis* infection.

Recently, we also reported that the IFN-γ activation induced by *H. suis* infection contributes to the production of CXCL13, which is directly associated with the formation of gastric lymphoid follicles (Yamamoto et al., 2014; Yang et al., 2015). In agreement, the mRNA expression levels of *Ifng* and *Cxcl13* in the gastric mucosa of *H. suis*-infected WT and *Myd88* KO mice at 6 months after infection were significantly increased compared with those in the gastric mucosa of *Trif* KO and *Myd88*/*Trif* DKO mice (Figures 1C and 1D). In addition, our previous study demonstrated a decrease in the number of *H. suis* bacteria in the stomachs of infected mice in proportion to the activation of IFN-γ (Yang et al., 2015), as IFN-γ is critical for the control of *Helicobacter* infection during the adaptive phase of immune responses (Harris et al., 2005; Mimura et al., 2011). Here, immunostaining and quantitative reverse transcription-PCR (qRT-PCR) results indicated that the number of *H. suis* bacteria was higher in the stomachs of *Trif* KO and *Myd88*/*Trif* DKO mice than in those of the WT and *Myd88* KO mice (Figures 1E and 1F). In addition, immunostaining analysis showed that *H. suis* was mainly located in the gastric mucosa of infected WT and *Myd88* KO mice, but not in *Trif* KO and *Myd88*/*Trif* DKO mice (Figure 1E), suggesting an inverse relationship between bacterial load and *Ifng* expression.

### TLR4 signaling activation is involved in gastric lymphoid follicle formation after *H. suis* infection

At 6 months after infection, *Tlr4* expression in the mouse stomach was detected with qRT-PCR and immunofluorescence staining. Compared with that in the uninfected mice, *Tlr4* mRNA expression was upregulated in the stomachs of both infected WT and *Myd88* KO mice, but not in infected *Trif* KO and *Myd88*/*Trif* DKO mice (Figure 2A). Moreover, immunostaining results indicated that TLR4 was mainly localized in the gastric mucosa of *H. suis*-infected WT and *Myd88* KO mice but not in gastric lymphoid follicles (Figure 2B). To further confirm the upregulation of TLR4 in the mouse stomach after *H. suis* infection, we performed fluorescence-activated cell sorting (FACS) analysis. Epithelial cell adhesion molecule (EpCAM), a marker of gastric epithelial tissues, was detected in the gastric epithelium of mice after *Helicobacter*
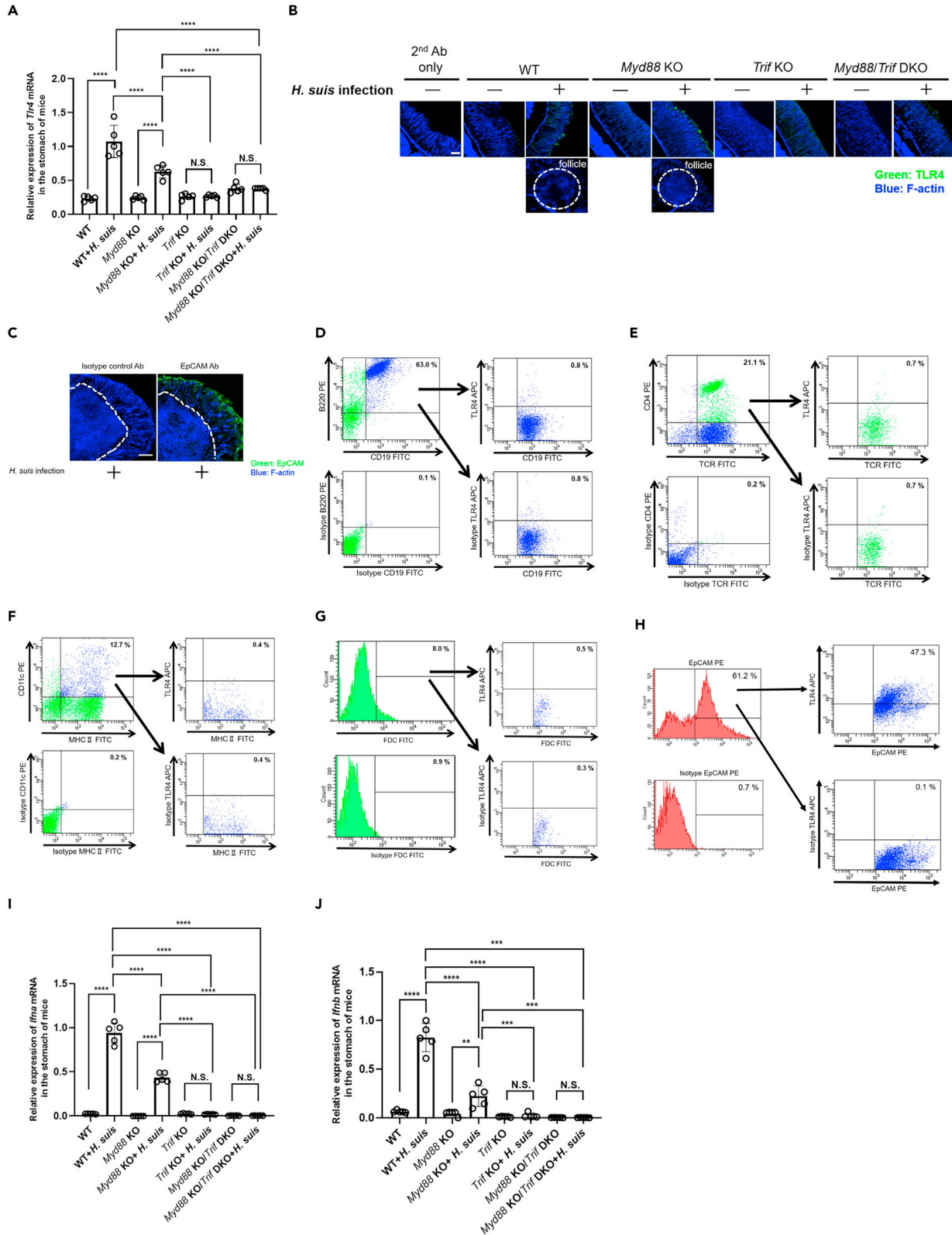
**A**



**B**



H. suis infection

follicle    follicle

Green: TLR4
Blue: F-actin

**C**



Isotype control Ab    EpCAM Ab

H. suis infection    +    +

Green: EpCAM
Blue: F-actin

**D**



**E**



**F**



**G**



**H**



**I**



**J**

**Figure 2. Activation of the TLR4 signaling pathway after _H. suis_ infection**

(A) _Tlr4_ mRNA levels in the stomachs of _H. suis_-infected WT, _Myd88_ KO, _Trif_ KO, and _Myd88/Trif_ DKO mice 6 months after infection were determined with qRT-PCR.

(B) Immunohistology of TLR4-expressing cells analyzed with confocal microscopy. Magnification, 100×.

(C) Immunohistology of EpCAM-positive cells in the stomachs of _H. suis_-infected WT mice. Magnification, 100×. Formation of gastric lymphoid follicles is indicated by dotted lines. Representative images are shown.

(D–H) C57BL/6J WT mice were infected with _H. suis_ for 6 months and gastric cells were analyzed with flow cytometry. (D) Staining with B220 and CD19 antibodies, followed by staining for TLR4. Right panels show TLR4 staining among B220 + CD19 + cells. (E) Staining with CD4 and TCRβ antibodies, followed by staining for TLR4. Right panels show TLR4 staining among CD4+ TCRβ+ cells. (F) Staining for CD11c and MHC class antibodies, followed by staining for TLR4. Right panels show TLR4 staining among CD11c + MHC class + cells.(G) Staining for FDC M1, followed by staining for TLR4. Right panels show TLR4 staining among FDC M1+ cells. (H) Staining for EpCAM, followed by staining for TLR4. Right panels show TLR4 staining among EpCAM + cells.

_Ifna_ (I) and _Ifnb_ (J) mRNA levels in the stomach after _H. suis_ infection were determined with qRT-PCR. (A, I, and J) Data were normalized to β-actin levels. Data are shown as the mean ± SD (n = 5) of three independent experiments. **p < 0.01, N.S., no significant difference (ANOVA). Ab, antibody; DKO, double knockout. Scale bar, 100 μm.

infection (Figure 2C) (Shibata et al., 2010; El-Zaatari et al., 2013; Lina et al., 2013; Shigematsu et al., 2013). Our results demonstrate that TLR4 activation was higher in the gastric epithelial cells after _H. suis_ infection than in other cells (Figures 2D–2H). In addition, _Ifna_ and _Ifnb_ mRNA expression levels were significantly increased in _H. suis_-infected WT and _Myd88_ KO mice compared with those in the respective uninfected animals; these changes were not observed in _Trif_ KO and _Myd88/Trif_ DKO mice (Figures 2I and 2J). These results suggest that the formation of gastric lymphoid follicles after _H. suis_ infection may be associated with activation of the TLR4–TRIF–type 1 IFN pathway.

## Monophosphoryl lipid A activates TLR4 on the gastric epithelium to induce type 1 IFN production

Bacterial monophosphoryl lipid A (MPLA) can induce type 1 IFNs via the activation of TLR4–TRIF signaling (Mata-Haro et al., 2007). In particular, type 1 IFNs are produced from gastric epithelial cells following _H. pylori_ infection (Watanabe et al., 2010). To examine whether bacterial MPLA can upregulate _TLR4_ expression in gastric epithelial cells, a gastric epithelial cell line (AGS) was treated with MPLA and then assessed with qRT-PCR and enzyme-linked immunosorbent assay (ELISA) for type 1 _IFN_ expression in cells and culture media, respectively. We observed increased _TLR4_ expression in AGS cells after MPLA treatment in a time-dependent manner (Figure 3A), as well as high _TRIF_ expression; however, this upregulation was significantly inhibited by treatment with a TLR4 peptide inhibitor (Figures 3B and 3C). Moreover, _IFNA_ and _IFNB_ expression significantly increased, in a time-dependent manner, in MPLA-treated AGS cells compared with that in the untreated cells (Figures 3D and 3E). The production of IFN-α and IFN-β in the culture medium also increased after MPLA treatment, consistent with mRNA levels (Figures 3F and 3G). Furthermore, type 1 _IFN_ expression was inhibited by TLR4 inhibitor treatment (Figures 3H and 3I). These results indicate that bacterial MPLA induces the production of type 1 IFNs from gastric epithelial cells via the TLR4 pathway.

## Relationship between _Ifnr_ expression and IFN-γ production in gastric-infiltrating cells in the mouse stomach after _H. suis_ infection

We reported that gastric B cells are IFN-γ-producing cells that respond to _H. suis_ infection and contribute to the development of gastric lymphoid follicles after infection (Yang et al., 2015). Nguyen et al. (2002) reported that IFN-α and β can directly activate STAT4, which is required for IFN-γ production during viral infection in mice. Therefore, to assess the relationship between the activation of IFNARs and IFN-γ induction, we examined the expression of IFNARs on infiltrating cells in the stomachs of _H. suis_-infected mice using FACS. Infiltrating gastric follicular B cells but not CD4+ T cells, DCs, FDCs, and gastric epithelial cells, displayed high expression of _Ifnar1_ and _Ifnar2_ after _H. suis_ infection (Figures 4A–4E). Moreover, _Ifng_ and _Stat4_ expression increased in the gastric B cells of _H. suis_-infected mice compared with that in those of the uninfected mice (Figures 4F and 4G). In contrast, IFN-γ was not expressed by gastric epithelial cells after MPLA stimulation (Figure S1). These results suggest that following _H. suis_ infection, gastric follicular B cells exhibit increased expression of _Ifnar1_ and _Ifnar2_, which may be associated with IFN-γ production.

## IFN-γ is produced by gastric B cells upon type 1 IFN stimulation via IFNAR activation

We hypothesized that the activation of IFNAR signaling in B cells stimulated with type 1 IFNs is crucial for IFN-γ production from gastric B cells, which can induce the formation of gastric MALT lymphoma after
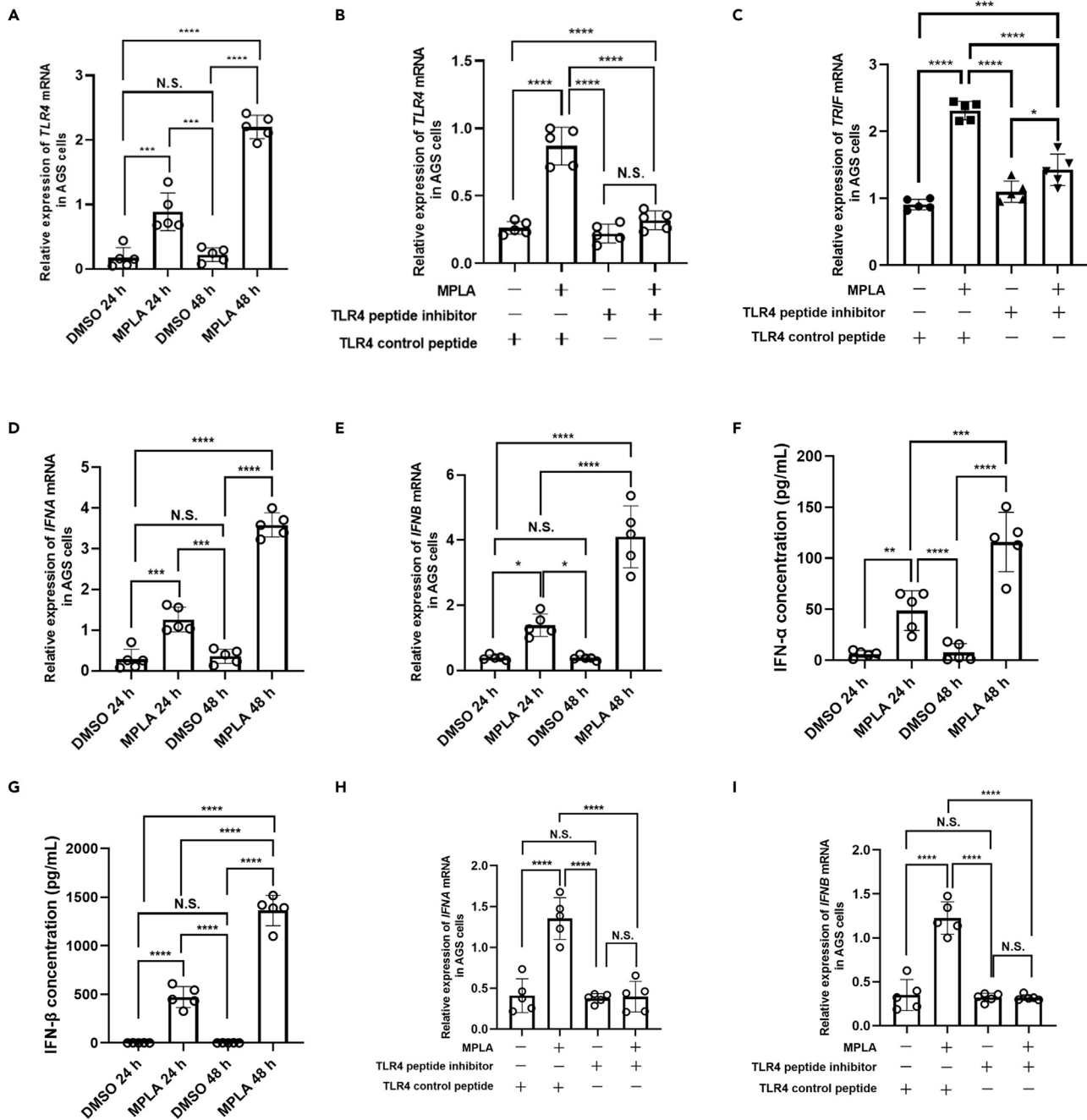
**Figure 3. Activation of TLR4 signaling in gastric epithelial cells after treatment with monophosphoryl lipid A (MPLA)**

Gastric epithelial cell lines (AGS cells) were treated with 1 μg/mL MPLA for 24 and 48 hr with or without the TLR4 inhibitor peptide (30 μM) 2 hr before MPLA treatment.

(A and B) qRT-PCR analysis of *TLR4* mRNA levels in AGS cells after treatment with MPLA at 24 and 48 hr (A) and with or without the TLR4 inhibitor at 48 hr (B).

(C–E) (C) qRT-PCR analysis of *TRIF* mRNA levels in AGS cells after treatment with MPLA, with or without the TLR4 inhibitor, after 48 hr qRT-PCR analysis of *IFNA* (D) and *IFNB* (E) expression levels in AGS cells at 24 and 48 hr after MPLA treatment.

ELISA of IFN-α (F) and IFN-β (G) production in AGS cells at 24 and 48 hr after MPLA treatment.

qRT-PCR analysis of *IFNA* (H) and *IFNB* (I) mRNA levels at 48 hr after MPLA treatment with or without the TLR4 inhibitor.

Data are shown as the mean ± SD (n = 5) of three independent experiments. qRT-PCR data were normalized to β-actin levels *p < 0.05, **p < 0.01, ****p < 0.0001, N.S., no significant difference (ANOVA).
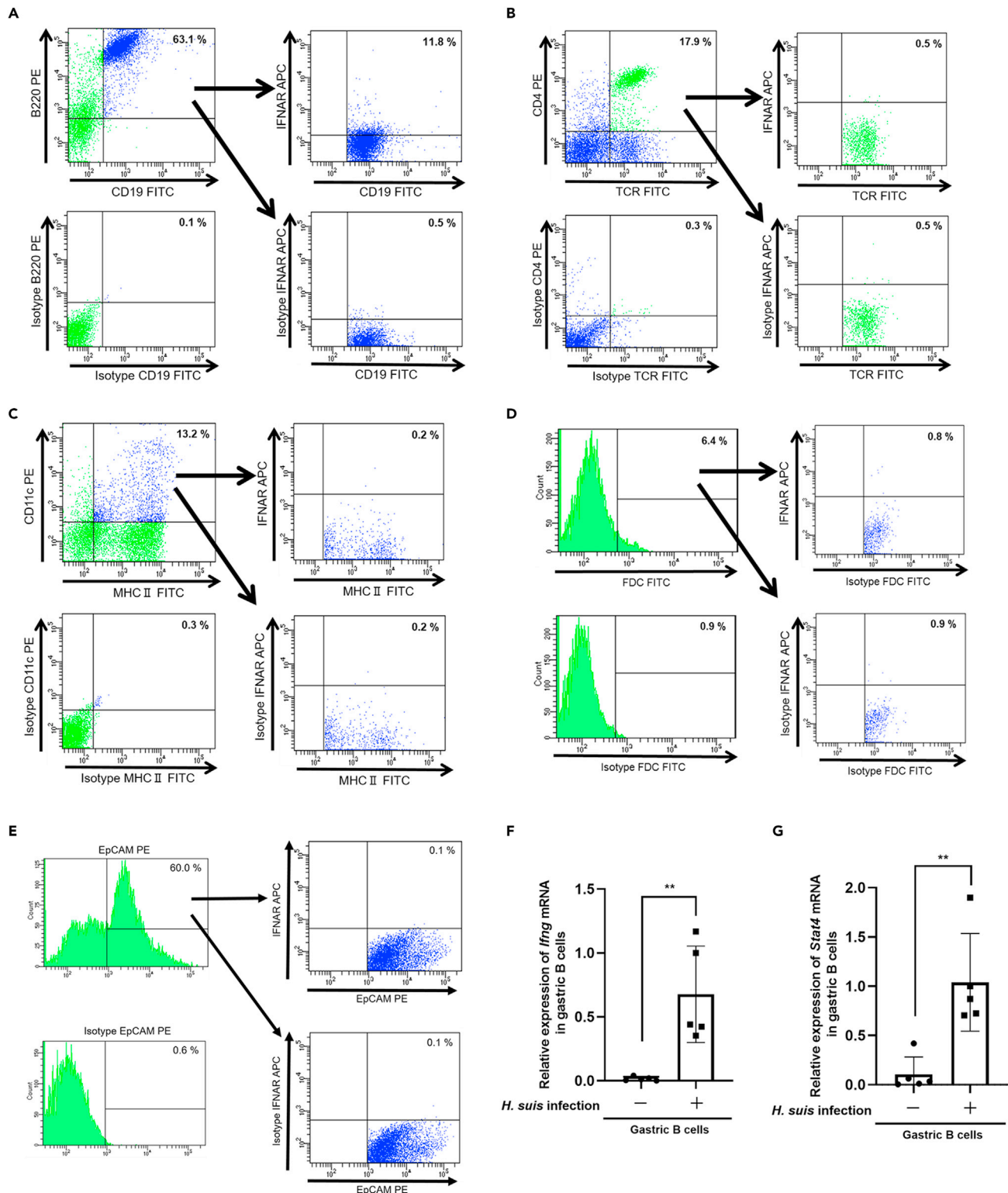
**Figure 4. Activation of IFNARs in cells infiltrating the stomachs of mice 6 months after *H. suis* infection**

C57BL/6J WT mice were infected with *H. suis* for 6 months and gastric cells were collected after enzymatic dissociation and gated for the appropriate population based on forward and side scatter; doublets were excluded.

(A) Staining for B220 and CD19 antibodies, followed by staining for IFNAR. Right panels show IFNAR staining and isotype control results among B220 + CD19 + cells.

**Figure 4.** *Continued*

(B) Staining for CD4 and TCRβ, followed by staining for IFNAR. Right panels show IFNAR staining and isotype control results among CD4+TCRβ+ cells.

(C) Staining for CD11c and MHC class antibodies, followed by staining for IFNAR. Right panels show IFNAR staining and isotype control results among CD11c + MHC class + cells.

(D) Staining for FDC M1, followed by staining for IFNAR. Right panels show IFNAR staining and isotype control results among FDC M1+ cells.

(E) Staining for EpCAM, followed by staining for IFNAR. Right panels show IFNAR staining and isotype control results among EpCAM + cells.

*Ifng* (F) and *Stat4* (G) mRNA levels in B cells isolated from the stomachs of WT mice with or without *H. suis* infection were determined with qRT-PCR and normalized to β-actin levels.

Data are shown as the mean ± SD (n = 5) of three independent experiments. **p < 0.01 (ANOVA). See also Figure S1.

*H. suis* infection. Accordingly, B cell lines were treated with recombinant type 1 IFNs, after which IFN-γ activation in B cells and secretion into the culture medium were detected with qRT-PCR and ELISA, respectively. *IFNG* expression and production increased after treatment with recombinant IFN-α (rIFN-α) or IFN-β (rIFN-β), but not MPLA (Figures 5A and 5B), and the combination of rIFN-α and rIFN-β synergistically enhanced IFN-γ production from B cells (Figures 5A and 5B); however, this upregulation was attenuated following IFNAR inhibition (Figures 5C and 5D). In addition, *STAT4* mRNA expression increased in response to type 1 IFN treatment in a time-dependent manner (Figure 5E), and phosphorylated STAT4 protein was also activated (Figure 5F), which is consistent with the expression pattern of *IFNG*. Moreover, the expression levels of *IFNAR* and IFN-γ receptors (*IFNGR*) significantly increased in response to rIFN-α and rIFN-β treatment compared with those in the untreated B cells (Figures 5G–5J); *IFNAR* was inhibited by an anti-IFNAR antibody (Figures 5K and 5L).

## IFN-γ activation is facilitated by positive feedback regulation of IFN-γ in B cells

The activation of IFNGRs expressed on B cells is under feedback regulation of IFNs (García-Sastre and Biron, 2006). Here, we found that IFNGRs were overexpressed on gastric B cells after *H. suis* infection (Figure 6A). In addition, *Ifngr1* and *Ifngr2* expression after *H. suis* infection (Figure 6B) was higher on purified gastric follicular B cells than on uninfected gastric B cells (Figures 6C and 6D). To examine whether the follicular B cells that infiltrated the stomachs of *H. suis*-infected mice produce IFN-γ via positive feedback, lymphoma B cell lines were treated with recombinant IFN-γ (rIFN-γ) for 24 or 48 hr. Using qRT-PCR and ELISA to detect IFN-γ gene and protein expression, respectively, we found that rIFN-γ-stimulated B cells secreted IFN-γ via positive feedback in a time-dependent manner (Figures 6E and 6F), and that IFNGR blockade inhibited IFN-γ production from B cells (Figures 6G and 6H). Similarly, *IFNGR1* and *IFNGR2* expression increased with rIFN-γ treatment in a time-dependent manner (Figures 6I and 6J) and was inhibited by an anti-IFNGR antibody (Figures 6K and 6L). These results indicate that IFN-γ production from B cells is enhanced by positive feedback-based regulation of IFN-γ, which may facilitate gastric lymphoid follicle formation after *H. suis* infection.

## DISCUSSION

In this study, we revealed that the production of type 1 IFNs from the gastric epithelium, via activation of the TLR4–TRIF pathway after *H. suis* infection, induces IFN-γ production from gastric B cells and the formation of gastric lymphoid follicles, ultimately leading to gastric MALT lymphoma. Previously, a study on T cell clones isolated from gastric MALT lymphoma showed that *H. pylori*-specific CD4^{+} T cells are important for the activation and proliferation of mucosal B cells in this disease (D'Elios et al., 1999). In addition, tumor-infiltrating T cells in MALT lymphoma appeared defective in both perforin-mediated cytotoxicity and Fas-mediated apoptosis despite displaying normal Fas ligand expression (D'Elios et al., 1999). However, our previous reports have shown that gastric MALT lymphoma formation after *H. suis* infection is T cell-independent (Yang et al., 2015). In fact, *H. suis* infection induces gastric lymphoid follicle formation in mice concomitant with high expression of *Ifng* in gastric B cells, independently of T cells (Yang et al., 2015).

Therefore, *H. pylori*- and *H. suis*-induced gastric MALT lymphomas appear to rely on different mechanisms. Moreover, the mechanism of IFN-γ production after *H. suis* infection underlying gastric MALT lymphoma formation remains unclear.

To date, various studies have reported that IFN production via TLR signaling is important for immune responses against viral and bacterial infections, providing further evidence of the link between innate and adaptive immunity (Bogdan et al., 2004; Theofilopoulos et al., 2005). However, TLR signaling is also
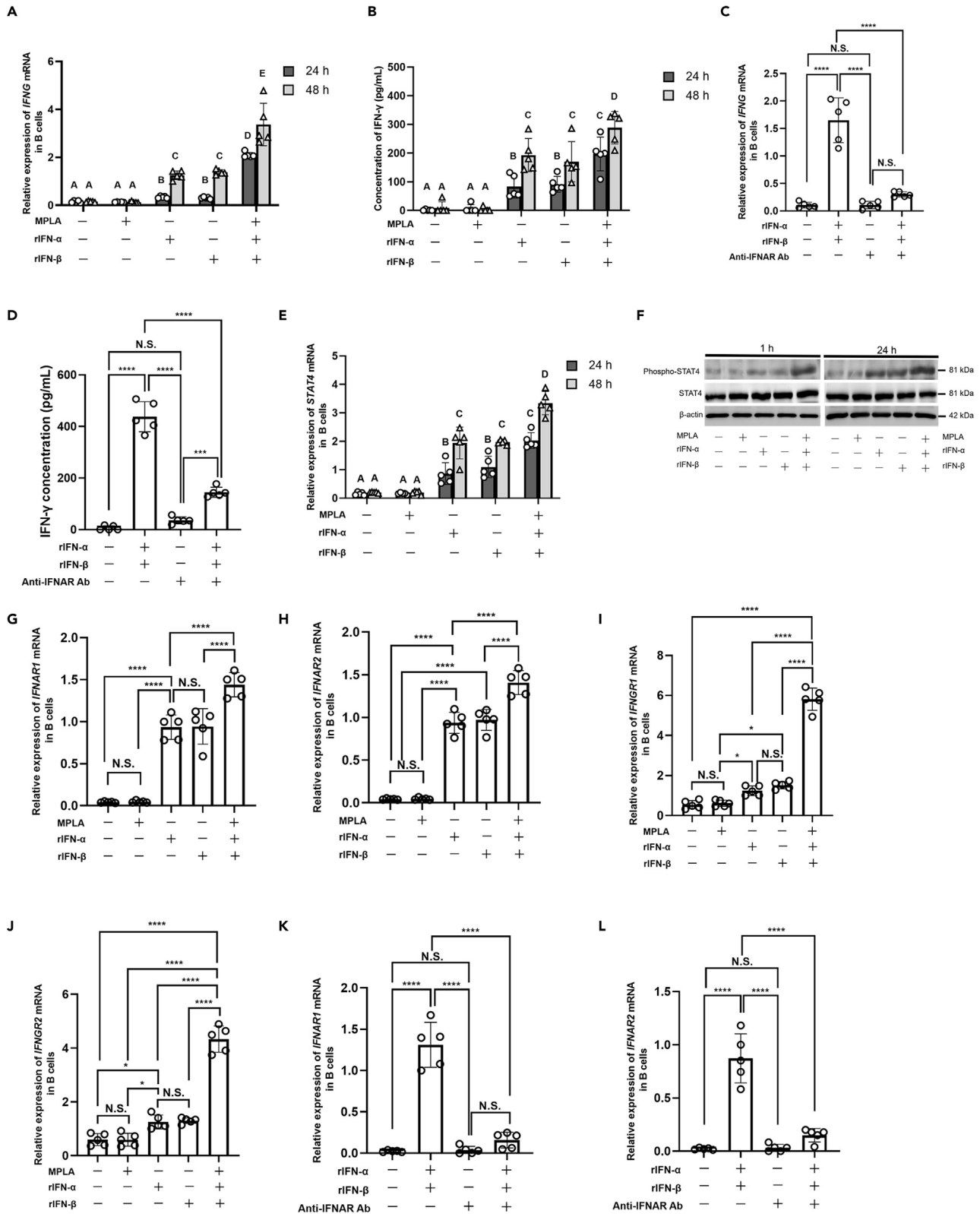
**Figure 5. IFN-γ production from B cells is enhanced by type 1 IFN stimulation via IFNAR activation**

(A and B) (A) qRT-PCR analysis of *IFNG* in Toledo cells (B cell lymphoma cell line) after treatment with rIFN-α, rIFN-β, and MPLA at 24 and 48 hr (B) ELISA of IFN-γ production by B cells after treatment with rIFN-α, rIFN-β, and MPLA at 24 and 48 hr. Toledo cells were treated with or without an anti-IFNAR antibody (5 μg/mL) 2 hr before rIFN-α and rIFN-β stimulation.

(C) qRT-PCR analysis of *IFNG* mRNA levels in B cells 48 hr after rIFN-α and rIFN-β treatment with or without an anti-IFNAR antibody.

(D) ELISA of IFN-γ production from B cells 48 hr after rIFN-α and rIFN-β treatment with or without an anti-IFNAR antibody.

(E) qRT-PCR analysis of *STAT4* expression levels in B cells after treatment with rIFN-α, rIFN-β, and MPLA at 24 and 48 hr (A, B, and E) Values with the same letters are not significantly different (Student's *t*-test; $p < 0.05$).

(F) Toledo cells were stimulated with rIFN-α, rIFN-β, and MPLA for 1 or 24 hr, followed by western blotting with antibodies specific for phosphorylated STAT4 or STAT4 and β-actin.

qRT-PCR analysis of *IFNAR1* (G), *IFNAR2* (H), *IFNGR1* (I), and *IFNGR2* (J) expression levels in B cells after treatment with rIFN-α, rIFN-β, and MPLA at 24 and 48 hr qRT-PCR analysis of *IFNAR1* (K) and *IFNAR2* (L) mRNA levels in B cells 48 hr after rIFN-α and rIFN-β treatment with or without an anti-IFNAR antibody. *$p < 0.05$, **$p < 0.01$, ***$p < 0.001$, ****$p < 0.0001$, N.S., not significant (ANOVA or Student's *t*-test).

Data are shown as the mean ± SD (n = 5) of three independent experiments. qRT-PCR data were normalized to β-actin levels.

implicated in disease exacerbation (Banchereau and Pascual, 2006; Banerjee et al., 2014). Therefore, IFN production is considered to exhibit dual roles: anti-microbial activity and disease promoting activity. The TLR4/TRIF pathway is also important for inducing type 1 IFNs in the stomachs of *Myd88* KO mice and contributes to the development and progression of gastric neoplasia upon *Helicobacter* infection (Banerjee et al., 2014). Similar to these reports, we demonstrated that the formation of gastric MALT lymphoma after *H. suis* infection is closely associated with TRIF pathway activation (Figure 1A) and that TLR4 is highly expressed in the gastric mucosa of *H. suis*-infected WT and *Myd88* KO mice but not in *Trif* KO mice (Figures 2A, 2B, and 2H). It has been reported that MALT-type gastric extranodal marginal zone B cell lymphomas exclusively express TLR4 (Adam et al., 2008); however, in this study, TLR4 was mainly expressed in the gastric mucosa, particularly in gastric B cells, but not in gastric lymphoid follicles. The *H. suis*-infected mouse model used in this study was analyzed 6 months after infection, suggesting that the time interval between infection and gastric MALT lymphoma formation is short. Given that the number of gastric lymphoid follicles in this model increases as the infection period elapses (Yamamoto et al., 2011) and that *H. suis* infection also exists in gastric MALT lymphoma in the human stomach (Okumura et al., 2013), the *H. suis* infection model employed has the potential to develop gastric MALT lymphoma; however, gastric MALT lymphoma formation should be pathologically evaluated using a mouse model with long-term infection (≥ 1 year). The above-mentioned findings suggest the importance of the TLR4–TRIF pathway in the early stages of gastric MALT lymphoma formation after *H. suis* infection.

Bacterial MPLA predominantly activates the TRIF pathway, leading to type 1 IFN production (Mata-Haro et al., 2007). Nguyen et al. (2002) reported that STAT4 activation via type 1 IFNs is required for IFN-γ production. Moreover, the IFN receptors, such as IFNARs and IFNGRs, expressed on B cells are associated with the production of IFNs via positive feedback regulation (Harris et al., 2005). We, thus, speculated that type 1 IFNs may be selectively involved in IFN-γ production from gastric epithelial cells after stimulation with MPLA derived from *H. suis*. We found that type 1 IFNs are mainly produced by gastric epithelial cells after stimulation with bacterial MPLA (Figures 3C–3F) and are associated with the activation of TLR4 signaling (Figures 3G and 3H). Moreover, IFNARs were expressed on infiltrating gastric follicular B cells but not on other cells in the stomachs of *H. suis*-infected mice (Figures 4A–4E), indicating that stimulation by type 1 IFNs enhances the production of IFN-γ from B cells via IFNAR–STAT4 signaling (Figure 5A–5L). These findings suggest that the type 1 IFNs produced by gastric epithelial cells after MPLA stimulation interact with IFNARs expressed on gastric follicular B cells, contributing to the induction of an IFN-γ response.

In contrast, several reports indicate that type 1 IFNs promote cell survival (Yang et al., 2000, 2001) and can induce anti-apoptotic effects (Sakamoto et al., 2005). In fact, our immunostaining data indicated that apoptotic cells were not detected in gastric lymphoid follicles after *H. suis* infection (Figure S2). Therefore, we speculate that the type 1 IFN-mediated stimulation of gastric follicular B cells has an anti-apoptotic effect, which enables the persistent infiltration of cells in the stomach and may facilitate the formation of gastric MALT lymphoma following *H. suis* infection. In addition, B cells are reported to produce IFN-γ via a T cell-independent pathway, initiating a positive feedback loop controlled by the IFN-γ receptor that stimulates B cells to persistently secrete IFN-γ (Harris et al., 2005). Similarly, our data demonstrate that IFN-γ production from gastric follicular B cells is facilitated by the positive feedback of B cells via IFN-γ receptors (Figures 6E–6H). These results suggest that after *H. suis* infection,
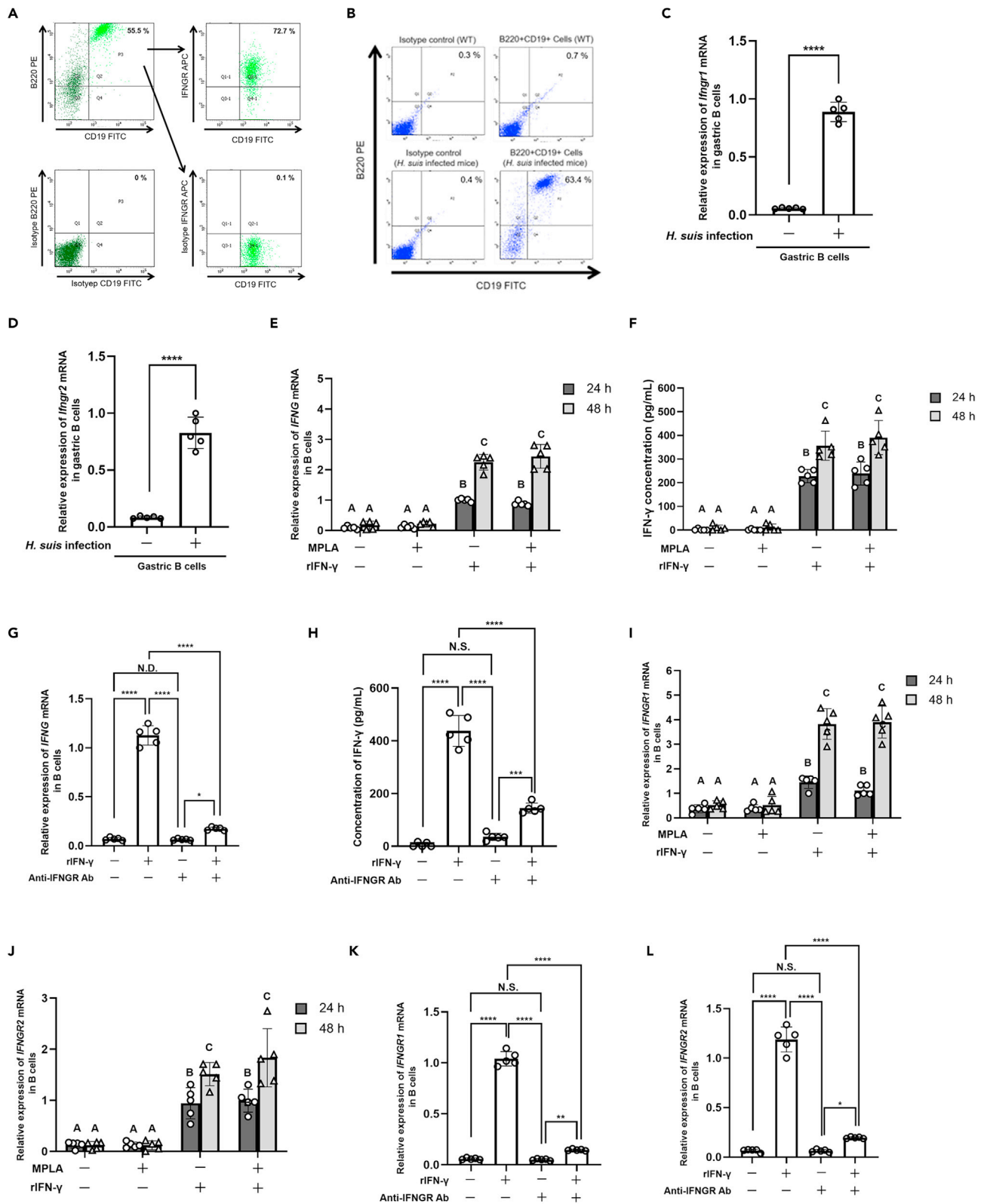
**Figure 6. IFN-γ production from B cells is enhanced by positive feedback regulation of IFN-γ**

(A) WT mice were infected with *Helicobacter suis* for 6 months and gastric cells were collected and stained with B220 and CD19 antibodies followed by staining for IFNGR. After gating for the appropriate population based on forward and side scatter, doublets were excluded. Right panels show IFNGR staining among B220 + CD19 + cells.

(B) FACS purification of B cells from the *H. suis*-infected stomachs of WT mice. Lymphocyte populations were determined based on forward and side scatter. Doublets were excluded and propidium iodine (PI)-negative (live) cells were selected for further analysis with specific antibodies to purify CD19 + B220 + cells. Isotype controls are also shown.

qRT-PCR analysis of *Ifngr1* (C) and *Ifngr2* (D) mRNA levels in gastric B cells. B cells were stimulated by MPLA and/or rIFN-γ at 48 hr. After stimulation, cells were washed and plated on dishes for 24 or 48 hr without stimulation.

*IFNG* expression (E) and production (F) following stimulation were determined with qRT-PCR and ELISA, respectively. Toledo cells were treated with or without an anti-IFNGR antibody (20 μg/mL) 2 hr before rIFN-γ stimulation.

(G) qRT-PCR analysis of *IFNG* mRNA levels in B cells 48 hr after IFN-γ treatment with or without an anti-IFNGR antibody.

(H) ELISA of IFN-γ production from B cells 48 hr after IFN-γ treatment with or without an anti-IFNGR antibody.

qRT-PCR analysis of *IFNGR1* (I) and *IFNGR2* (J) expression levels in B cells after stimulation with IFN-γ.

qRT-PCR analysis of *IFNGR1* (K) and *IFNGR2* (L) expression levels in B cells 48 hr after IFN-γ treatment with or without an anti-IFNGR antibody.

(C–L) Data are shown as mean ± SD (n = 5). *$p < 0.05$, **$p < 0.01$, ***$p < 0.001$, ****$p < 0.0001$, N.S., not significant (ANOVA or Student's *t*-test). Values with the same letters are not significantly different (Student's *t*-test; $p < 0.05$). qRT-PCR data were normalized to β-actin levels.

gastric follicular B cells are activated to produce IFN-γ and are involved in gastric MALT lymphoma development.

We recently reported that the B lymphocyte chemoattractant CXCL13 is crucial for the formation of gastric MALT lymphoma after *H. suis* infection (Yang et al., 2015). Moreover, its expression is inhibited in *Ifng*-KO mice after *H. suis* infection (Mimura et al., 2011). Interestingly, our results suggest that IFN-γ can induce the production of CXCL13 by FDCs (Figure S3).

In conclusion, our findings suggest that gastric epithelial cells produce type 1 IFNs through the TLR4–TRIF pathway, which is activated via interactions between bacterial MPLA and IFNAR expressed on gastric B cells. Moreover, gastric B cells are under feedback regulation of type 1 IFN and produce IFN-γ to facilitate gastric MALT lymphoma formation after *H. suis* infection. Therefore, IFNAR-positive gastric follicular B cells may be crucial for the formation of gastric MALT lymphoma after *H. suis* infection. Based on our study outcomes, we propose blocking type 1 IFNs and IFNARs as a novel targeted therapy for suppressing the formation of lymphomas, such as gastric MALT lymphoma, after *H. suis* infection.

## Limitations of the study

One limitation of this study is that we did not use animal models to determine whether the IFN-γ produced following *H. suis* infection stimulates FDCs and is directly associated with gastric MALT lymphoma formation. Our preliminary results showed that stimulation of purified mouse FDCs with rIFN-γ induced the expression of CXCL13 in these cells (Figure S3), suggesting that IFN-γ produced in the stomachs of *H. suis*-infected mice interacts with FDCs and drives CXCL13 production. However, further studies are warranted to determine the direct relevance of FDCs. Another limitation of our study is that although we provided an evidence that IFN-γ is involved in developing gastric MALT lymphoma following *H. suis* infection, whether inhibition of IFN-γ production can suppress the development of gastric MALT lymphoma in humans after *H. suis* infection remains unclear. We presumed that *H. suis* infection comprises multiple steps leading to the development of gastric lymphoid follicles. Moreover, IFN-γ produced by gastric follicular B cells has been suggested as a key factor controlling gastric MALT lymphoma formation. As such, IFN treatment can protect against microorganism infection (Cooper et al., 1993; Huang et al., 1993; Perry et al., 1997); however, high doses of IFN may facilitate the formation of several lymphomas, including gastric MALT lymphoma. Therefore, although regulating IFN-γ production after *H. suis* infection is critical for inhibiting gastric MALT lymphoma formation, the pathway that must be blocked to achieve this remains unknown. Thus, to determine the appropriate pathway to target, neutralizing antibodies should be employed against the signaling pathways involved in IFN-γ production in *H. suis*-infected animal models; this would help develop strategies for suppressing IFN-γ production and inhibiting gastric MALT lymphoma formation.

## STAR★METHODS

Detailed methods are provided in the online version of this paper and include the following:

## SUPPLEMENTAL INFORMATION

Supplemental information can be found online at https://doi.org/10.1016/j.isci.2021.103064.

## AUTHOR CONTRIBUTIONS

K.Y. and N.S. designed the project. K.Y. and Y.K. performed the experiments, performed FACS analysis and *in vitro* experiments, and contributed to data-related discussions. K.Y. performed the animal experiments. Y.K. and M.Y. provided essential materials and contributed to data-related discussions. K.Y., S.O., Y.K., T.S., and N.S. interpreted the experimental data. K.Y., S.O., Y.K., and T.S. wrote the manuscript. N.S. critically revised the manuscript and supervised the study.

## DECLARATION OF INTERESTS

The authors declare no competing interests.

## REFERENCES

Adam, P., Schmausser, B., Göbeler-Kolve, M., Müller-Hermelink, H.K., and Eck, M. (2008). Gastric extranodal marginal zone B-cell lymphomas of MALT type exclusively express Toll-like receptor 4 in contrast to other lymphomas infiltrating the stomach. Ann. Oncol. *19*, 566–569.

Aderem, A., and Ulevitch, R.J. (2000). Toll-like receptors in the induction of the innate immune response. Nature *406*, 782–787.

Asahi, K., Fu, H.Y., Hayashi, Y., Eguchi, H., Murata, H., Tsujii, M., Tsuji, S., Tanimura, H., and Kawano, S. (2007). *Helicobacter pylori* infection affects Toll-like receptor 4 expression in human gastric mucosa. Hepatogastroenterology *54*, 1941–1944.

Baele, M., Decostere, A., Vandamme, P., Ceelen, L., Hellemans, A., Mast, J., Chiers, K., Ducatelle, R., and Haesebrouck, F. (2008). Isolation and characterization of *Helicobacter suis* sp. nov. from pig stomachs. Int. J. Syst. Evol. Microbiol. *58*, 1350–1358.

Banchereau, J., and Pascual, V. (2006). Type I interferon in systemic lupus erythematosus and other autoimmune diseases. Immunity *25*, 383–392.

Banerjee, A., Thamphiwatana, S., Carmona, E.M., Rickman, B., Doran, K.S., and Obonyo, M. (2014). Deficiency of the myeloid differentiation primary response molecule MyD88 leads to an early and rapid development of *Helicobacter*-induced gastric malignancy. Infect. Immun. *82*, 356–363.

Ben Suleiman, Y., Yoshida, M., Nishiumi, S., Tanaka, H., Mimura, T., Nobutani, K., Yamamoto, K., Takenaka, M., Aoganghua, A., Miki, I., et al. (2012). Neonatal Fc receptor for IgG (FcRn)

expressed in the gastric epithelium regulates bacterial infection in mice. Mucosal Immunol. *5*, 87–98.

Bogdan, C., Mattner, J., and Schleicher, U. (2004). The role of type I interferons in non-viral infections. Immunol. Rev. *202*, 33–48.

Cooper, A.M., Dalton, D.K., Stewart, T.A., Griffin, J.P., Russell, D.G., and Orme, I.M. (1993). Disseminated tuberculosis in interferon gamma gene-disrupted mice. J. Exp. Med. *178*, 2243–2247.

D'Elios, M.M., Amedei, A., Manghetti, M., Costa, F., Baldari, C.T., Quazi, A.S., Telford, J.L., Romagnani, S., and Del Prete, G. (1999). Impaired T-cell regulation of B-cell growth in *Helicobacter pylori*-related gastric low-grade MALT lymphoma. Gastroenterology *117*, 1105–1112.

El-Zaatari, M., Kao, J.Y., Tessier, A., Bai, L., Hayes, M.M., Fontaine, C., Eaton, K.A., and Merchant, J.L. (2013). Gli1 deletion prevents *Helicobacter*-induced gastric metaplasia and expansion of myeloid cell subsets. PLoS One *8*, e58935.

García-Sastre, A., and Biron, C.A. (2006). Type 1 interferons and the virus-host relationship: a lesson in détente. Science *312*, 879–882.

Hansen, F.C., Kalle-Brune, M., van der Plas, M.J., Strömdahl, A.C., Malmsten, M., Mörgelin, M., and Schmidtchen, A. (2015). The thrombin-derived host defense peptide GKY25 inhibits endotoxin-induced responses through interactions with lipopolysaccharide and macrophages/monocytes. J. Immunol. *194*, 5397–5406.

Harris, D.P., Goodrich, S., Gerth, A.J., Peng, S.L., and Lund, F.E. (2005). Regulation of IFN-gamma production by B effector 1 cells: essential roles for T-bet and the IFN-gamma receptor. J. Immunol. *174*, 6781–6790.

Hoshino, K., Takeuchi, O., Kawai, T., Sanjo, H., Ogawa, T., Takeda, Y., Takeda, K., and Akira, S. (1999). Cutting edge: toll-like receptor 4 (TLR4)-deficient mice are hyporesponsive to lipopolysaccharide: evidence for TLR4 as the *Lps* gene product. J. Immunol. *162*, 3749–3752.

Huang, S., Hendriks, W., Althage, A., Hemmi, S., Bluethmann, H., Kamijo, R., Vilcek, J., Zinkernagel, R.M., and Aguet, M. (1993). Immune response in mice that lack the interferon-gamma receptor. Science *259*, 1742–1745.

Imler, J.L., and Hoffmann, J.A. (2001). Toll receptors in innate immunity. Trends Cell Biol. *11*, 304–311.

Lina, T.T., Pinchuk, I.V., House, J., Yamaoka, Y., Graham, D.Y., Beswick, E.J., and Reyes, V.E. (2013). CagA-dependent downregulation of B7-H2 expression on gastric mucosa and inhibition of Th17 responses during *Helicobacter pylori* infection. J. Immunol. *191*, 3838–3846.

Mata-Haro, V., Cekic, C., Martin, M., Chilton, P.M., Casella, C.R., and Mitchell, T.C. (2007). The vaccine adjuvant monophosphoryl lipid A as a

TRIF-biased agonist of TLR4. Science *316*, 1628–1632.

Medzhitov, R., and Janeway, C.A., Jr. (1998). An ancient system of host defense. Curr. Opin. Immunol. *10*, 12–15.

Mimura, T., Yoshida, M., Nishiumi, S., Tanaka, H., Nobutani, K., Takenaka, M., Suleiman, Y.B., Yamamoto, K., Ota, H., Takahashi, S., et al. (2011). IFN-gamma plays an essential role in the pathogenesis of gastric lymphoid follicles formation caused by *Helicobacter suis* infection. FEMS Immunol. Med. Microbiol. *63*, 25–34.

Nakamura, M., Murayama, S.Y., Serizawa, H., Sekiya, Y., Eguchi, M., Takahashi, S., Nishikawa, K., Takahashi, T., Matsumoto, T., Yamada, H., et al. (2007). "*Candidatus* Helicobacter heilmannii" from a cynomolgus monkey induces gastric mucosa-associated lymphoid tissue lymphomas in C57BL/6 mice. Infect. Immun. *75*, 1214–1222.

Nakao, Y., Funami, K., Kikkawa, S., Taniguchi, M., Nishiguchi, M., Fukumori, Y., Seya, T., and Matsumoto, M. (2005). Surface-expressed TLR6 participates in the recognition of diacylated lipopeptide and peptidoglycan in human cells. J. Immunol. *174*, 1566–1573.

Nguyen, K.B., Watford, W.T., Salomon, R., Hofmann, S.R., Pien, G.C., Morinobu, A., Gadina, M., O'Shea, J.J., and Biron, C.A. (2002). Critical role for STAT4 activation by type 1 interferons in the interferon-gamma response to viral infection. Science *297*, 2063–2066.

Okumura, T., Iwaya, Y., Yokosawa, S., Suga, T., Arakura, N., Matsumoto, T., Ogiwara, N., Higuchi, K., Ota, H., and Tanaka, E. (2013). A case of *Helicobacter heilmannii*-associated primary gastric mucosa-associated lymphoid tissue lymphoma achieving complete remission after eradication. Clin. J. Gastroenterol. *6*, 38–45.

O'Rourke, J.L., Solnick, J.V., Neilan, B.A., Seidel, K., Hayter, R., Hansen, L.M., and Lee, A. (2004). Description of '*Candidatus* Helicobacter heilmannii' based on DNA sequence analysis of 16S rRNA and urease genes. Int. J. Syst. Evol. Microbiol. *54*, 2203–2211.

Perry, L.L., Feilzer, K., and Caldwell, H.D. (1997). Immunity to *Chlamydia trachomatis* is mediated by T helper 1 cells through IFN-gamma-dependent and -independent pathways. J. Immunol. *158*, 3344–3352.

Priestnall, S.L., Wiinberg, B., Spohr, A., Neuhaus, B., Kuffer, M., Wiedmann, M., and Simpson, K.W. (2004). Evaluation of "*Helicobacter heilmannii*" subtypes in the gastric mucosa of cats and dogs. J. Clin. Microbiol. *42*, 2144–2151.

Sakamoto, E., Hato, F., Kato, T., Sakamoto, C., Akahori, M., Hino, M., and Kitagawa, S. (2005). Type I and type II interferons delay human neutrophil apoptosis via activation of STAT3 and up-regulation of cellular inhibitor of apoptosis 2. J. Leukoc. Biol. *78*, 301–309.

Schmausser, B., Andrulis, M., Endrich, S., Lee, S.K., Josenhans, C., Müller-Hermelink, H.K., and Eck, M. (2004). Expression and subcellular distribution of toll-like receptors TLR4, TLR5 and TLR9 on the gastric epithelium in *Helicobacter pylori* infection. Clin. Exp. Immunol. *136*, 521–526.

Shibata, W., Takaishi, S., Muthupalani, S., Pritchard, D.M., Whary, M.T., Rogers, A.B., Fox, J.G., Betz, K.S., Kaestner, K.H., Karin, M., et al. (2010). Conditional deletion of IkappaB-kinase-beta accelerates *Helicobacter*-dependent gastric apoptosis, proliferation, and preneoplasia. Gastroenterology *138*, 1022–1034.

Shigematsu, Y., Niwa, T., Rehnberg, E., Toyoda, T., Yoshida, S., Mori, A., Wakabayashi, M., Iwakura, Y., Ichinose, M., Kim, Y.J., et al. (2013). Interleukin-1beta induced by *Helicobacter pylori* infection enhances mouse gastric carcinogenesis. Cancer Lett. *340*, 141–147.

Takeda, K., and Akira, S. (2005). Toll-like receptors in innate immunity. Int. Immunol. *17*, 1–14.

Theofilopoulos, A.N., Baccala, R., Beutler, B., and Kono, D.H. (2005). Type I interferons (alpha/beta) in immunity and autoimmunity. Annu. Rev. Immunol. *23*, 307–336.

Watanabe, T., Asano, N., Fichtner-Feigl, S., Gorelick, P.L., Tsuji, Y., Matsumoto, Y., Chiba, T., Fuss, I.J., Kitani, A., and Strober, W. (2010). NOD1 contributes to mouse host defense against *Helicobacter pylori* via induction of type I IFN and activation of the ISGF3 signaling pathway. J. Clin. Invest. *120*, 1645–1662.

Yamamoto, K., Nishiumi, S., Yang, L., Klimatcheva, E., Pandina, T., Takahashi, S., Matsui, H., Nakamura, M., Zauderer, M., Yoshida, M., et al. (2014). Anti-CXCL13 antibody can inhibit the formation of gastric lymphoid follicles induced by *Helicobacter* infection. Mucosal Immunol. *7*, 1244–1254.

Yamamoto, K., Tanaka, H., Nishitani, Y., Nishiumi, S., Miki, I., Takenaka, M., Nobutani, K., Mimura, T., Ben Suleiman, Y., Mizuno, S., et al. (2011). *Helicobacter suis* KB1 derived from pig gastric lymphoid follicles induces the formation of gastric lymphoid follicles in mice through the activation of B cells and CD4 positive cells. Microbes Infect *13*, 697–708.

Yang, C.H., Murti, A., Pfeffer, S.R., Basu, L., Kim, J.G., and Pfeffer, L.M. (2000). IFNalpha/beta promotes cell survival by activating NF-kappa B. Proc. Natl. Acad. Sci. U S A *97*, 13631–13636.

Yang, C.H., Murti, A., Pfeffer, S.R., Kim, J.G., Donner, D.B., and Pfeffer, L.M. (2001). Interferon alpha/beta promotes cell survival by activating nuclear factor kappa B through phosphatidylinositol 3-kinase and Akt. J. Biol. Chem. *276*, 13756–13761.

Yang, L., Yamamoto, K., Nishiumi, S., Nakamura, M., Matsui, H., Takahashi, S., Dohi, T., Okada, T., Kakimoto, K., Hoshi, N., et al. (2015). Interferon-gamma-producing B cells induce the formation of gastric lymphoid follicles after *Helicobacter suis* infection. Mucosal Immunol. *8*, 279–295.

## STAR★METHODS

### KEY RESOURCES TABLE

| REAGENT or RESOURCE | SOURCE | IDENTIFIER |
|---|---|---|
| Antibodies | | |
| Polyclonal rabbit anti-*Helicobacter pylori* | DAKO | Cat#B047129-1; RRID: AB_2313773 |
| Purified rat anti-mouse CD45R | BD Biosciences | Cat#553086; RRID: AB_394616 |
| Purified rat anti-mouse CD4 | BD Biosciences | Cat#550280; RRID: AB_393575 |
| Purified rat anti-mouse F4/80 | BD Biosciences | Cat#565409; RRID: AB_2739222 |
| Purified anti-mouse NK-1.1 | BioLegend | Cat#108702; RRID: AB_313389 |
| PE rat anti-mouse CD45R/B220 | BD Biosciences | Cat#553089; RRID: AB_394619 |
| PE rat IgG2a, κ isotype control | BD Biosciences | Cat#553930; RRID: AB_479719 |
| FITC rat anti-mouse CD19 | BD Biosciences | Cat#553785; RRID: AB_395049 |
| FITC rat IgG2a κ isotype control | BD Biosciences | Cat#553929; RRID: AB_395144 |
| PE rat anti-mouse CD4 | BD Biosciences | Cat#553049; RRID: AB_394585 |
| FITC hamster anti-mouse TCR β | BD Biosciences | Cat#553171; RRID: AB_394683 |
| FITC hamster IgG2, λ1 isotype control | BD Biosciences | Cat#553964; RRID: AB_395165 |
| FITC hamster anti-mouse CD11c | BD Biosciences | Cat#553801; RRID: AB_395060 |
| PE hamster anti-mouse CD11c | BD Biosciences | Cat#557401; RRID: AB_396684 |
| PE hamster IgG1, λ1 isotype control | BD Biosciences | Cat#553954; RRID: AB_395158 |
| FITC rat anti-mouse I-A/I-E | BD Biosciences | Cat#553623; RRID: AB_394958 |
| Purified rat anti-mouse follicular dendritic cell | BD Biosciences | Cat#551320; RRID: AB_394151 |
| FITC goat anti-rat Ig | BD Biosciences | Cat#554016; RRID: AB_395210 |
| Monoclonal rat anti-mouse Ep-CAM (G8.8) | BioLegend | Cat#118202; RRID: AB_1089026 |
| PE rat anti-mouse CD326 | BD Biosciences | Cat#563477; RRID: AB_2738233 |
| Polyclonal rabbit anti-TLR4 | Abcam | Cat#ab13556; RRID: AB_300457 |
| APC-conjugated anti-mouse TLR4 | BioLegend | Cat#145406; RRID: AB_2562502 |
| Biotin-conjugated anti-mouse TLR4 | Abcam | Cat#ab6788; RRID: AB_954885 |
| DyLight 488-conjugated streptavidin | Jackson ImmunoResearch Laboratories, Inc | Cat#016-480-084; RRID: AB_2313773 |
| APC-conjugated anti-mouse IFNAR1 | BioLegend | Cat#127314; RRID: AB_2122745 |
| Biotin hamster anti-mouse CD119 | BD Biosciences | Cat#550482; RRID: AB_393698 |
| Biotin hamster IgG1, κ isotype control | BD Biosciences | Cat#553970; RRID: AB_395170 |
| APC streptavidin | BD Biosciences | Cat#554067; RRID: AB_10050396 |
| Alexa Fluor 488-conjugated anti-mouse NK1.1 | BioLegend | Cat#108718; RRID: AB_2658317 |
| Alexa Fluor 488 mouse IgG2a, κ isotype ctrl antibody | BioLegend | Cat#400233; RRID: AB_2313773 |
| p-Stat4 (Y693) rabbit Ab | Cell Signaling Technology | Cat#5267S; RRID: AB_10545446 |
| Stat4 (C46B10) rabbit mAb | Cell Signaling Technology | Cat#2653S; RRID: AB_2255156 |
| Monoclonal anti-β-actin antibody | Sigma-Aldrich | Cat#A5441; RRID: AB_476744 |
| Purified rat anti-mouse CD16/CD32 | BD Biosciences | Cat#553142; RRID: AB_394657 |
| Goat anti-rat IgG (H + L) cross-adsorbed secondary antibody, Alexa Fluor 488 | Thermo Fisher Scientific | Cat#A-11006; RRID: AB_2534074 |
| Goat anti-rat IgG (H + L) cross-adsorbed secondary antibody, Alexa Fluor 546 | Thermo Fisher Scientific | Cat#A-11081; RRID: AB_141738 |
| Goat anti-rabbit IgG (H + L) cross-adsorbed secondary antibody, Alexa Fluor 488 | Thermo Fisher Scientific | Cat#A-11008; RRID: AB_143165 |

*Continued*

| REAGENT or RESOURCE | SOURCE | IDENTIFIER |
|---|---|---|
| Goat anti-mouse IgG (H + L)-HRP conjugate | Bio-Rad Laboratories, Inc. | Cat#1721011; RRID: AB_261713 |
| Goat anti-rabbit IgG (H + L)-HRP conjugate | Bio-Rad Laboratories, Inc. | Cat#1706515; RRID: AB_2617112 |
| **Bacterial and virus strains** | | |
| *Helicobacter suis* | Isolated from pig | NA |
| **Chemicals, peptides, and recombinant proteins** | | |
| Recombinant human IFN-alpha A/D | R&D Systems, Inc. | Cat#11200-2 |
| Recombinant human IFN-beta 1a | R&D Systems, Inc. | Cat#11410-2 |
| MPLA-SM | Thermo Fisher Scientific | Cat#tlrl-mpla |
| TLR4 inhibitor peptide set | Novus Biologicals | Cat#NBP2-26244 |
| 7-AAD | BD Biosciences | Cat#559925 |
| Propidium iodide staining solution | BD Biosciences | Cat#556463 |
| Alexa Fluor 647 phalloidin | Thermo Fisher Scientific | Cat#A22287 |
| **Critical commercial assays** | | |
| Human IFN-a Multi-Subtype ELISA Kit | Thermo Fisher Scientific | Cat#411051 |
| Human IFN beta ELISA Kit | Thermo Fisher Scientific | Cat#41410-1 |
| IFN-$\gamma$ human ELISA Kit | Thermo Fisher Scientific | Cat#EHIFNG |
| Mammalian Whole cell protein extraction Kit | PromoCell GmbH | Cat#PK-CA577-K269 |
| **Experimental models: cell lines** | | |
| Human: Toledo | American Type Culture Collection | ATCC: CRL-2631 |
| Human: AGS | American Type Culture Collection | ATCC: CRL-1739 |
| **Experimental models: Organisms/Strains** | | |
| Mouse: WT: C57BL/6J | CLEA Japan Inc. | C57BL/6JJcl |
| Mouse: WT: C57BL/6J | Japan SLC | C57BL/6JJmsSlc |
| Mouse: *Myd88* KO: *Myd88* deficient | Oriental Yeast Co., Ltd. | B6.129-Myd88$^{tm1Aki}$/Obs RRID: IMSR_OBS:1 |
| Mouse: *Trif* KO: *Trif* deficient | Oriental Yeast Co., Ltd. | B6.129P2-Trif$^{tm1Aki}$/Obs IMSR_OBS:16 |
| Mouse: *Myd88/Trif* DKO: *Myd88/Trif* deficient | Oriental Yeast Co., Ltd. | B6.129P2-MyD88/Trif$^{tm1Aki}$/Obs RRID: IMSR_OBS:22 |
| **Oligonucleotides** | | |
| Primers for qPCR, see Table S2 | This paper | N/A |
| **Software and algorithms** | | |
| GraphPad Prism 8.2.0 | GraphPad Software | https://www.graphpad.com/scientific-software/prism/ |
| BD FACSDiva v8.0.1 Software | BD Biosciences | https://www.bdbiosciences.com/us/instruments/research/software/flow-cytometry-acquisition/bd-facsdiva-software/m/111112/features |
| LSM Image Browser | Carl Zeiss Co. Ltd | https://www.embl.de/eamnet/html/body_image_browser.html |
| DP Controller 2.2.1.227 | Olympus Corporation | N/A |
| ImageQuant LAS4000 Mini Version 1.2 Build 1.2.2.127 | GE Healthcare Life Sciences | N/A |

**Continued**

| REAGENT or RESOURCE | SOURCE | IDENTIFIER |
|---|---|---|
| Other | | |
| ImageQuant LAS 4000 | GE Healthcare Life Sciences | 28955810 |
| LSM710 | ZEISS | N/A |
| Olympus BX51 | Olympus Corporation | N/A |
| BD FACSArialII | BD Biosciences | N/A |
| ABI 7300 Real-Time PCR System | Thermo Fisher Scientific | N/A |
| iMark Microplate Absorbance Reader | Bio-Rad Laboratories, Inc. | N/A |

## RESOURCE AVAILABILITY

### Lead contact

Further information and requests for resources and reagents should be directed to and will be fulfilled by the lead contact, Koji Yamamoto (kyama@pop.med.hokudai.ac.jp).

### Materials availability

This study did not generate new unique reagents.

### Data and code availability

- All data reported in this paper will be shared by the lead contact upon request.

- This paper does not report original code.

- Any additional information required to reanalyze the data reported in this paper is available from the lead contact upon request.

## EXPERIMENTAL MODEL AND SUBJECT DETAILS

### Mice

All animal experiments were performed according to the Guidelines for Animal Experimentation at Kobe University (Permission No. P130105 and P130106) and Hokkaido University (Permission No. 17-0094) and the ARRIVE guidelines. C57BL/6J mice (age- and sex-matched groups) were purchased from CLEA Japan (C57BL/6JJcl; Tokyo, Japan) and Japan SLC (C57BL/6JJmsSlc; Shizuoka, Japan). *Myd88* KO (IMSR_OBS:1), *Trif* KO (IMSR_OBS:16), and *Myd88/Trif* DKO mice (IMSR_OBS:1) of C57BL/6 background (age- and sex-matched groups) were purchased from Oriental Bioservice (Kyoto, Japan). All mice were maintained under barrier conditions in microisolator cages containing either compressed paper or aspen chip bedding placed on free-standing shelves or in individually ventilated cage racks. All KO mice were co-housed to homogenize their gut microbiota. The animals were maintained under specific pathogen-free conditions in a clean room with controlled environment at the Institute for Animal Experimentation, Hokkaido University Graduate School of Medicine, or at Kobe University Graduate School of Medicine. The temperature was maintained at $22 \pm 3°C$ with a 12 hr light/dark cycle. All mice had unlimited access to standard chow and water.

### H. suis infection

Six-week-old female C57BL/6J, *Myd88* KO, *Trif* KO, and *Myd88/Trif* DKO mice were infected with *H. suis*. *In vitro* cultivation of *H. suis* has been previously reported (Baele et al., 2008); however, this bacterium has not been successfully cultivated in our laboratory. The infectious *H. suis* was originally obtained from a pig stomach (Yamamoto et al., 2011) and maintained in the stomachs of C57BL/6J mice for 3 to 6 months after the infection (as donors). These methods have already been established and used in several studies (Mimura et al., 2011; Ben Suleiman et al., 2012; Yamamoto et al., 2014; Yang et al., 2015). We previously reported that *Helicobacter* species, other than *H. suis,* are not found to colonize the stomachs of donor mice (Yamamoto et al., 2011). After 12 hr of fasting, the same amount of gastric mucosal homogenates from donors was orally administered to each group of mice, while the control mice were administered an equal volume of PBS.

### Cell culture and *in vitro* experiments

Toledo cells (CRL-2631; female human lymphoma cell line) and AGS cells (CRL-1739; female human gastric carcinoma cell line) were purchased from the American Type Culture Collection (Manassas, VA, USA). The cells were cultured in RPMI 1640 medium (30,264-85; Nacalai Tesque Inc., Kyoto, Japan), supplemented with 10% fetal calf serum, 2 mM L-glutamine, 1.5 g/L sodium bicarbonate, and 4.5 g/L glucose, at 37°C and 5% $CO_2$. AGS cells were stimulated with recombinant human IFN-alpha A/D (11,200-2; R&D Systems, Minneapolis, MN, USA) at 9,000 U/mL, recombinant human IFN-beta 1a (11,410-2; R&D Systems) at 9,000 U/mL, recombinant human IFN-γ (285-IF-100; R&D Systems) at 1 μg/mL, TLR4 inhibitor peptide (NBP2-26244; Novus Biologicals, Centennial, CO, USA) at 30 μM, control peptide (NBP2-26244; Novus Biologicals) at 30 μM, and MPLA-SM (tlrl-mpla; Invitrogen, Carlsbad, CA, USA) at 10 μg/mL for 24 or 48 hr. After stimulation, the cells were collected for qRT-PCR analysis, and the culture supernatants were collected for IFN measurement using ELISA.

## METHOD DETAILS

### Histological examination

Six months after *H. suis* infection, all mice were sacrificed by cervical dislocation under anesthesia. The stomachs were resected and opened at the outer curvature and sliced longitudinally from the esophagus to the duodenum. Half of the stomach was embedded in paraffin, while one-quarter was used for RNA extraction. The remaining portion was frozen in the Tissue-Tek OCT Compound (Sakura Finetek, Tokyo, Japan). The paraffin-embedded tissues were longitudinally sliced (three slices) and stained with hematoxylin and eosin. Every section from each sample included both the corpus and antrum. The number of gastric MALT lymphomas was counted in the three slices from each mouse and determined in a blinded manner.

### Immunofluorescence staining

Immunohistochemical analysis was carried out using frozen tissue sections obtained from the stomachs of mice at 12 weeks after *H. suis* infection and antibody treatment. The sections were air-dried, fixed in acetone for 5 min, and blocked with 10% goat serum for 30 min. After washing with PBS, the sections were incubated with the appropriate antibodies overnight at 4°C before incubation with the corresponding secondary antibodies for 60 min at room temperature as previously described (Yamamoto et al., 2014; Yang et al., 2015). The sections were imaged using a confocal laser-scanning microscope (LSM 5 Pascal; Zeiss, Oberkochen, Germany) and analyzed using the LSM Image Browser with a 10× objective. All antibodies used in this study are listed in Table S1.

### Enzymatic dissociation of gastric cells

The infiltrated cells in non-infected and *H. suis*-infected mouse stomachs were isolated as previously described (Yang et al., 2015), with some modifications. Briefly, the stomachs were resected, washed in cold PBS, stored in collection medium (calcium- and magnesium-free HBSS containing 5% FBS and 1% penicillin plus streptomycin), cut into small pieces, rinsed in collection medium containing 1 mM dithiothreitol and 1 mM EDTA, and agitated at 100 rpm for 1 hr at 37°C. Epithelial cells were pelleted by centrifugation of the medium, and collected. The stomach tissues were washed with RPMI 1640 medium and then treated with 1 mg/mL collagenase (Sigma-Aldrich, St. Louis, MO, USA) in RPMI 1640 medium, supplemented with 10% FBS and 1% penicillin plus streptomycin, at 37°C for 3 hr under agitation. Undigested tissues were removed by filtration, and the cells were resuspended in cold stain buffer to maintain the concentration at $2 \times 10^7$ cells/mL for staining.

### Antibody staining and cell isolation using FACS

The cells collected using the method described in "Enzymatic dissociation of gastric cells" were treated with propidium iodide or 7-aminoactinomycin D staining solution (559,925; BD Biosciences, San Jose, CA, USA) to identify viable cells. Appropriate antibodies or their isotype control antibodies (Table S1) were added at an optimal concentration and incubated for 30 min on ice in the dark. B cells were stained with anti-B220 and anti-CD19 antibodies; T cells with anti-CD4 and anti-TCR antibodies; and DCs with anti-aCD11c and anti-MHCII antibodies. Gastric epithelial cells were stained with an anti-EpCAM antibody. For FDC labeling, the cells were first stained with an anti-FDC-M1 antibody on ice for 1 hr, followed by FITC-conjugated goat anti-rat IgG. Finally, the cells were stained with anti-IFNAR, anti-TLR4, or anti-IFNGR antibodies, washed with buffer to remove unbound antibodies, resuspended at a final concentration of $2 \times 10^7$ cells/mL, and analyzed on a BD FACSAria III cell sorter to collect the purified B cells.

## qRT-PCR

RNA was isolated from homogenates, stomach-isolated cells, and cultured cells using TRIzol Reagent (15596-018; Invitrogen) and then reverse-transcribed into cDNA using the High-Capacity cDNA Reverse Transcription Kit (4368813; Applied Biosystems, Foster City, CA, USA) according to the manufacturer's instructions. qRT-PCR was performed using the Power SYBR Green PCR Master Mix on an ABI Prism 7500 Real-Time PCR system (Applied Biosystems) according to the manufacturer's instructions. To compare relative gene expression levels, the comparative $C_T$ ($2^{-\Delta\Delta Ct}$) method was used, and measurements were normalized to those of β-actin cDNA as an endogenous control. All primers (Hokkaido System Science, Sapporo, Japan) used in this study are listed in Table S2.

## Measurement of IFN production

Cell culture supernatants were collected and analyzed for IFN-α, IFN-β, and IFN-γ production using an IFN-α (411051), IFN-β (41410-1), or IFN-γ (EHIFNG) Human ELISA Kit (Thermo Fisher Scientific, Waltham, MA, USA), respectively, according to the manufacturer's instructions.

## Western blotting

Protein extracts were prepared using the Mammalian Whole Cell Protein Extraction Kit (PK-CA577-K269; PromoCell, Heidelberg, Germany). The lysates were subjected to sodium dodecyl sulfate-polyacrylamide gel electrophoresis and subsequently electro-transferred onto nitrocellulose membranes. The membranes were blocked with Blocking One-P (05999-84; Nacalai Tesque) or Blocking One (03953-95; Nacalai Tesque) and treated with primary antibodies against phosphorylated STAT4, STAT4, and β-actin, followed by incubation with horseradish peroxidase-conjugated anti-mouse (1721011) or anti-rabbit (1706515; Bio-Rad Laboratories, Hercules, CA, USA) IgG secondary antibodies. The immunoblots were developed using the ChemiLumiONE (07880; Nacalai Tesque) or SuperSignal West Dura Extended Duration Substrate (34076; Thermo Fisher Scientific) and visualized using an Image Reader (LAS-4000 Imaging System; Fujifilm, Tokyo, Japan).

## QUANTIFICATION AND STATISTICAL ANALYSIS

All results are expressed as mean ± standard deviation (SD). Statistical significance was analyzed using the Student's t-test for comparisons between two groups and one-way ANOVA for comparisons among more than three groups. GraphPad Prism 8.2.0 was used for data analysis. $p < 0.05$ was considered statistically significant. The number of mice or samples used for each experiment is indicated in each figure legend.